Saturation of the Paramagnetic Resonance of a V Center*

T. G. CASTNER, JR.†
Physics Department, University of Illinois, Urbana, Illinois
(Received April 16, 1959)

The saturation of the paramagnetic resonance of the $(\text{halogen})_2^-$ complex (V_K center) in the alkali halides has been studied. The saturation of the absorption signal ($\chi''H_1$) *versus* H_1 is obtained over a 60-db power range for KCl, KBr, and LiF at 78°K. Portis' theory of inhomogeneous saturation has been generalized by omitting the assumption that the individual spin packet width is very much smaller than the envelope width. Methods are developed to determine independently from a given experimental saturation curve the spin-packet width $1/T_2$, the spin-lattice relaxation time T_1, and the product T_1T_2. For KCl and LiF values of T_2, T_1 and T_1T_2 are determined for the different hyperfine lines of the V_K center spectrum. For KBr only the product T_1T_2 could be obtained. From the results it is concluded that the spin-packet width is not limited by T_1. For KCl at 78°K, $T_1 \sim 7T_2$; for LiF, T_2 is two orders of magnitude or more less than T_1 and depends in a complicated manner on the external magnetic field and the angle between the V_K center axis and the external field.

INTRODUCTION

EXPERIMENTALLY measured electron spin-lattice relaxation times have not generally been in quantitative agreement with calculated spin-lattice relaxation times for electron spins in metals, semiconductors, and insulators. In some cases the agreement is sufficiently poor that it is uncertain what is the dominant mechanism responsible for the coupling between the spins and the phonons. A particularly interesting system for spin-lattice relaxation studies is the V_K center,[1] the first hole-type color center in alkali halides discovered by paramagnetic resonance techniques. There are several reasons why this center is more attractive for the study of paramagnetic relaxation than many other paramagnetic systems: (1) The electronic structure of the V_K center is known quite accurately.[2] The wave function (mostly p orbital), the principal g values, the hyperfine coupling constants, and the electronic excited states are well known for this center in LiF, KCl, KBr, and NaCl. These parameters are better known than for iron group paramagnetic ions (d orbitals) or rare earth paramagnetic ions (f orbitals). In addition, by forming the V_K centers in different alkali halides, these parameters can be varied which is a helpful method for sorting out relaxation mechanisms. (2) These centers are located in a simple cubic lattice. Moreover, extensive work has been done on the lattice dynamics of the alkali halides[3]—much more than on the often studied salts containing water of hydration. Furthermore, the V_K center (trapped hole) is a smaller perturbation on the lattice than other paramagnetic defects involving vacancies or interstitials. (3) The V_K center has an axis of symmetry and strongly anisotropic spin-orbit and hyperfine interactions. This makes it possible to check the orientation dependence of the spin-lattice relaxation times, another useful method for sorting out mechanisms. In addition, because of the well resolved hyperfine spectrum, relaxation times can be determined for different hyperfine lines. (4) Since the V_K centers can be formed by x-irradiation at 78°K, their concentration can be changed in a controlled manner. This fact allows one to investigate possible concentration-dependent spin-lattice relaxation effects in the same sample. (5) It is a one-electron-type defect.

The F center, on the other hand, is the best known paramagnetic color center and has also received the most attention. However, there are several reasons why the V_K center is more attractive for paramagnetic relaxation studies. The much greater localization of the wave function for the V_K center allows a simpler theoretical model for spin-lattice relaxation calculations. The lattice accommodating the trapped hole contains no vacancies. The narrow resonance line widths for the V_K center insure better signal to noise than for the F-center resonance and greatly reduce the problem of modulation fast passage effects. The details of the resonance spectrum of the V_K center may allow more information to be measured about relaxation processes, although double-resonance techniques for the F center[4] might offset this advantage. Nevertheless, it will be interesting to compare the V_K-center saturation behavior with the known results for the F center.

The F-center resonance static line width has been successfully attributed to the hyperfine interaction of the electron spin with nuclei surrounding the F-center halogen ion vacancy.[5] This broadening is of the inhomogeneous type due to the interaction of the electron spin with something outside the F-center electron spin

* Sponsored in part by the Alfred P. Sloan Foundation; it is part of a thesis submitted in partial fulfillment of the requirements for the degree of Doctor of Philosophy in Physics at the University of Illinois.
† Present address: General Electric Research Laboratory, Schenectady, New York.
[1] W. Känzig, Phys. Rev. **99**, 1890 (1955).
[2] T. G. Castner and W. Känzig, J. Phys. Chem. Solids **3**, 178 (1957); T. O. Woodruff and W. Känzig, J. Phys. Chem. Solids **5**, 268 (1958).
[3] M. Born and K. Huang, *Dynamical Theory of Crystal Lattices* (Clarendon Press, Oxford, 1954), Chap. II.
[4] G. Feher, Phys. Rev. **105**, 1122 (1957).
[5] Kip, Kittel, Levy, and Portis, Phys. Rev. **91**, 1066 (1953).

system. Portis[6] investigated the saturation behavior of the F center at room temperature showing that the dispersion component, χ', of the susceptibility did not saturate at all. The absorption component, χ'', of the susceptibility saturated, but in a different manner than a homogeneously broadened line, the susceptibility falling off only as $1/H_1$ rather than as $1/H_1^2$ for the homogeneous case.

The problem of inhomogeneous saturation was first treated by Bloembergen, Purcell, and Pound[7] for an inhomogeneous external magnetic field. Portis[6] developed the theory of saturation due to inhomogeneous broadening for both the dispersion and the absorption and successfully explained the experimental saturation behavior of the F center including the breakdown of the Kramers-Kronig relations connecting χ'' and χ'. Portis, from his F-center absorption saturation curve, determined the product of the longitudinal spin-lattice relaxation time, T_1, and the transverse or spin-dephasing time, T_2. However, he could not independently determine T_1 or T_2 without a further assumption about the spin-packet width. A spin packet is composed of all spins having the same static field to within a field interval determined by the dephasing time T_2. In any case, for the F center the inhomogeneity broadening producing the static width is several orders of magnitude larger than the individual spin-packet width.

The V_K center differs markedly from the single broad unresolved F-center resonance. The trapped hole resonance consists of a well-resolved hyperfine spectrum containing a large number of quite narrow lines. Analysis reveals the spectrum can be accounted for by assuming that it arises from a halogen molecule ion (e.g., Cl_2^- in KCl, F_2^- in LiF). A complete discussion of the electronic structure of the V_K center has been made by Känzig and the author,[2] hereafter referred to as "C and K." Their discussion reported that even the narrow V_K center lines (1.35 gauss in KCl) were Gaussian and likely inhomogeneously broadened by the hyperfine interaction of the hole with nuclei neighboring the molecule ion. The work below reports absorption saturation measurements on the V_K center electron-spin resonance (ESR) transitions and the determination of the individual spin-packet width $(1/\gamma T_2)$ and the longitudinal spin-lattice relaxation times at 78°K. Because of the narrow lines and the use of a high-power klystron, saturation curves could be obtained over a 60-db range in power. These curves for large power bent down like a homogeneously saturated resonance. Portis' saturation theory for inhomogeneously broadened lines has been extended to find a general expression for χ'' without making the assumption that the individual spin-packet width is very much less than the envelope width due to the inhomogeneous broadening. Making use of the general expression for χ'' and curve fitting techniques, values of the spin-packet width and T_1 were determined. It had been the bias of the author and others[8] to assume that the spin packet-width must be limited by T_1. However, the experimental saturation curves could only be explained by making T_1 longer than T_2. This work concludes that the spin-packet width is not determined by spin-lattice relaxation at 78°K. In addition, the results show that steady-state saturation methods may be used to extract the spin-packet width and spin-lattice relaxation of inhomogeneously broadened ESR transitions if the lines are narrow enough and sufficient microwave power is available. It is noted that the inhomogeneous saturation is a quite common and general phenomenon, and there are a large number of examples of inhomogeneously broadened ESR lines.[9]

Saturation of Homogeneously Broadened Lines

Saturation of homogeneously broadened lines is characterized by a uniform decrease of the susceptibility of the entire line independent of where the power is applied in the line. The line-broadening mechanism ensures that the microwave energy is absorbed by all the spins. Bloembergen[10] treats this case, and Portis[6] reviews it in his F-center saturation work. Following Bloembergen, we consider the case with the spin $S=\frac{1}{2}$, and let n be the surplus number of spins, $n=N_--N_+$, where N_- is the number of spins with $M_s=-\frac{1}{2}$ and N_+ is the number with $M_s=+\frac{1}{2}$. Then n has a thermal equilibrium value $n_0=(N_++N_-)g\beta H/2kT_L$, where g is the spectroscopic splitting factor, β is the Bohr magneton, H is the applied magnetic field, and T_L is the lattice temperature. The magnitude of n is determined by the competition between the applied power tending to saturate the ESR (making $n=0$) and the spin-lattice relaxation tending to restore the excess spin population to the thermal equilibrium value n_0. Thus

$$(dn/dt)_{\mathrm{rf}}=-\pi\gamma^2H_1^2g(\omega-\omega_0)n, \tag{1}$$

$$(dn/dt)_{\mathrm{SL}}=-(n-n_0)/T_1, \tag{2}$$

where γ is the gyromagnetic ratio, H_1 is the rotating component of the microwave magnetic field inducing transitions $(\Delta M_s=\pm1)$, $g(\omega-\omega_0)$ is the normalized shape function for the transition, and T_1 is the spin-

[6] A. M. Portis, Phys. Rev. **91**, 1071 (1953).
[7] Bloembergen, Purcell, and Pound, Phys. Rev. **73**, 679 (1948).
[8] A. M. Portis, Phys. Rev. **104**, 584 (1956); A. G. Redfield, Phys. Rev. **98**, 1787 (1955); C. P. Slichter (private discussion). More recently, Bloembergen, Shapiro, Pershan, and Artman, Phys. Rev. **114**, 445 (1959), discuss the problem of saturation of inhomogeneously broadened lines. They consider a spin-packet width $1/\gamma T_2$ and relaxation time T_1 and introduce a cross-relaxation time T_{21} determined by multiple spin flips or by random diffusion in frequency space. The time required for a spin to diffuse across a distribution of width $1/\gamma T_2^*$ is found to be T_2^4/T_2^{*3}.
[9] G. Feher, Phys. Rev. **114**, 1219 (1959); W. Känzig and T. O. Woodruff, J. Phys. Chem. Solids **9**, 70 (1958); Känzig finds that the H center saturates in a way indicating inhomogeneous broadening. Other paramagnetic color centers also show inhomogeneous saturation. See also J. L. Burkhardt, Phys. Rev. Letters **2**, 149 (1959).
[10] N. Bloembergen, Ph.D. thesis, Harvard University (Drukkerij Fa. Schotanus & Jens, Utrecht, 1948).

lattice relaxation time. For the stationary condition these two rates are equal, and the surplus number of spins n is given by

$$n=n_0\frac{1}{1+\pi\gamma^2H_1^2g(\omega-\omega_0)T_1}. \quad (3)$$

The rate at which power is absorbed from the microwave field is $P=\frac{1}{2}\hbar\omega(dn/dt)_{\rm rf}$, the $\frac{1}{2}$ appearing because one spin flip changes n by 2. Combining this with the relationship between the power absorbed by the sample and the absorption susceptibility (i.e., $P=\frac{1}{2}\omega\chi''H_1^2$), the absorption susceptibility resulting is

$$\chi''(\omega)=\tfrac{1}{2}\chi_0\omega_0\frac{\pi g(\omega-\omega_0)}{1+\pi\gamma^2H_1^2g(\omega-\omega_0)T_1}, \quad (4)$$

where the static susceptibility χ_0 is equal to $g^2\beta^2(N_++N_-)/4kT_L$. If T_2 for the homogeneous line is defined as in Portis' work; i.e., $g(0)=T_2/\pi$, this expression assumes the familiar Bloch form for the line center,

$$\chi''=\tfrac{1}{2}\chi_0\omega_0T_2\left(\frac{1}{1+\gamma^2H_1^2T_2T_1}\right). \quad (5)$$

The X-band spectrometer described below measures a signal $V_R\propto\chi''H_1$. Below saturation the signal is just proportional to the microwave field H_1, while for strong saturation of the homogeneously broadened line the signal $V_R\propto 1/H_1$. In this case the power absorbed from the rf field by the ESR transition becomes independent of H_1. The relative signal measured by the spectrometer has the form

$$V_R=X/(1+X^2), \quad (6)$$

where $X=\gamma H_1(T_1T_2)^{\frac{1}{2}}$. From a homogeneous saturation curve the value T_1T_2 may be experimentally determined, and knowledge of the homogeneous width $(1/\gamma T_2)$ allows one to find the spin-lattice relaxation time T_1. We now will compare this homogeneous saturation with inhomogeneous saturation.

Inhomogeneous Saturation

Inhomogeneous broadening of the ESR transition comes from those interactions outside the electron spin system which vary slowly over the time required for spin transitions. Only those spins with Larmor frequencies within $1/T_2$ or γH_1, whichever is larger, of the Larmor frequency $\omega=\gamma H$ satisfying the resonance condition will be saturated with sufficient microwave power. The spin packets precessing at different Larmor frequencies interact very weakly with each other, and spin diffusion[11] is extremely slow. Thus it is possible to "dig a hole" in the inhomogeneous line; that is, saturate only a narrow portion of the line, namely the width determined by H_1 or T_2.

In treating inhomogeneous saturation we must now distinguish between two frequency distributions; one $g(\omega-\omega')$, the line-shape function of the individual spin packet which is homogeneously broadened and very narrow, and two, the distribution of static fields $h(\omega-\omega_0)$ (centered about ω_0) providing the shape function or envelope of the distribution of spin packets. These are both normalized so that

$$\int_0^\infty g(\omega-\omega')d\omega'=1, \quad \int_0^\infty h(\omega'-\omega_0)d\omega'=1. \quad (7)$$

Following Portis[3] and implicitly assuming that the spin packets behave independently of each other and making use of (4), the absorption susceptibility becomes

$$\chi''(\omega)=\tfrac{1}{2}\chi_0\int_0^\infty\frac{\pi\omega'g(\omega-\omega')h(\omega-\omega_0)d\omega'}{1+\pi\gamma^2H_1^2T_1g(\omega-\omega')}. \quad (8)$$

Portis has shown the dispersion susceptibility to be

$$\chi'(\omega)=\tfrac{1}{2}\chi_0\int_0^\infty\frac{\omega'h(\omega'-\omega_0)d\omega'}{1+\pi\gamma^2H_1^2T_1g(\omega-\omega')}\times\int_0^\infty\frac{2\omega''g(\omega''-\omega')d\omega''}{\omega''^2-\omega^2}. \quad (9)$$

Portis then shows, for the case in which the over-all broadening is very large in comparison with the width of the spin packets, that these expressions become

$$\chi''(\omega)=\tfrac{1}{2}\chi_0\omega h(\omega-\omega_0)\int_0^\infty\frac{\pi g(\omega-\omega')d\omega'}{1+\pi^2H_1^2T_1g(\omega-\omega')}, \quad (10)$$

$$\chi'(\omega)=\tfrac{1}{2}\chi_0\int_0^\infty\frac{2\omega'^2h(\omega-\omega_0)d\omega'}{\omega'^2-\omega^2}. \quad (11)$$

Several important features should be noted. The expression for the dispersion is independent of the microwave field, H_1, and does not saturate. The absorption line shape is that of the envelope and is independent of the degree of saturation. The way in which χ'' saturates will depend on the line shape function of the individual spin packets. In particular, if the line shape is Lorentzian, the shape function will be

$$g(\omega-\omega')=\frac{T_2}{\pi}\frac{1}{1+T_2^2(\omega-\omega')^2}. \quad (12)$$

Performing the integration the absorption susceptibility will be given by

$$\chi''=\tfrac{1}{2}\chi_0\omega_0h(\omega-\omega_0)\frac{1}{(1+\gamma^2H_1^2T_1T_2)^{\frac{1}{2}}}, \quad (13)$$

[11] P. W. Anderson, Phys. Rev. **109**, 1492 (1958). Calculation of the spacial spin diffusion for the V_K center in concentrations of 10^{17}/cc using Anderson's result give a spin diffusion of order 0.1 second.

and the spectrometer absorption signal becomes

$$V_R \propto \chi'' H_1 \propto X/(1+X^2)^{\frac{1}{2}}, \tag{14}$$

where $X=\gamma H_1(T_1T_2)^{\frac{1}{2}}$. In this case the absorption signal increases linearly below saturation and then just flattens out for $X>1$.

In the saturation of the F-center resonance, Portis found that the dispersion signal did not saturate at all over a range of 50 or more in power. The absorption signal increased linearly and then flattened out in agreement with (14). In addition, Portis determined the value of T_1T_2 at room temperature. His results confirm that the individual spin-packet width is extremely narrow in comparison with the inhomogeneous broadening. In addition, the individual spin-packet line shape is closely Lorentzian. Portis emphasizes that if the spin-packet line shape fell off any more rapidly in the wings than a Lorentzian line, the absorption signal for $H_1>1/\gamma(T_1T_2)^{\frac{1}{2}}$ $(X>1)$ would decrease instead of flattening out. That the individual spin-packet line shape is Lorentzian will be the major assumption in extending Portis' theory.

The V_K center resonance lines are Gaussian and are inhomogeneously broadened, but the spin-packet width may be only an order of magnitude or so less than the inhomogeneous width, and it is no longer a good approximation to assume that $h(\omega-\omega_0)$ is slowly varying over a spin packet. From the results on the F center and the nature of the individual spin packet, one can conclude that the Lorentzian assumption seems a good one for the line shape of the individual spin packet. Hence, the normalized distributions are

$$g(\omega-\omega')=\frac{T_2}{\pi}\frac{1}{1+T_2^2(\omega-\omega')^2}, \tag{15}$$

$$h(\omega'-\omega_0)=\frac{1}{\pi^{\frac{1}{2}}}\frac{1}{\Delta\omega_G}\exp\left[-\left(\frac{\omega'-\omega_0}{\Delta\omega_G}\right)^2\right], \tag{16}$$

where $\Delta\omega_G$ is the Gaussian width of the inhomogeneous broadening. (The width between points of maximum slope of the absorption, χ'', is $\Delta H_{\text{max slope}}=\sqrt{2}\Delta\omega_G/\gamma$.) The T_2 of the homogeneous Lorentzian line is defined by the condition $\Delta\omega_L T_2=1$, where $\Delta\omega_L$ is the frequency width for half maximum of $g(\omega)$ for the individual spin packet. The absorption susceptibility becomes, from (8),

$$\chi''(\omega)=\frac{\frac{1}{2}\chi_0}{\pi^{\frac{1}{2}}\Delta\omega_L\Delta\omega_G}\times\int_0^\infty\frac{\omega'\exp[-(\omega'-\omega_0)^2/(\Delta\omega_G)^2]d\omega'}{1+[(\omega-\omega')^2/\Delta\omega_L]+(\gamma^2H_1^2T_1/\Delta\omega_L)}. \tag{17}$$

In general, this integral is difficult to evaluate, but it can be solved for $\omega=\omega_0$; that is, the susceptibility may be calculated at the line center. This has been done in Appendix A. The result is

$$\chi''(\omega_0)=\tfrac{1}{2}\chi_0\pi^{\frac{1}{2}}\left(\frac{\omega_0}{\Delta\omega_G}\right)\frac{\exp(a^2t^2)}{t}[1-\Phi(at)], \tag{18}$$

where $\Phi(at)$ is the error function, a is a parameter which measures the degree of inhomogeneous broadening, namely the ratio $\Delta\omega_L/\Delta\omega_G$ of the Lorentzian spin-packet width to the inhomogeneous Gaussian width, and $t=(1+\gamma^2H_1^2T_1T_2)^{\frac{1}{2}}$ is a saturation factor. The relative spectrometer absorption signal is proportional to $\chi''H_1$ and can be written

$$V_R=\frac{X}{(1+X^2)^{\frac{1}{2}}}\exp(a^2X^2)\frac{\{1-\Phi[a(1+X^2)^{\frac{1}{2}}]\}}{[1-\Phi(a)]}. \tag{19}$$

As the parameter a approaches zero, the expression for V_R approaches Eq. (14) corresponding to the F-center case where the individual spin-packet width is negligible compared to the inhomogeneous broadening. Figure 1 shows the spectrometer signal V_R plotted *versus* X or $H_1/H_{\frac{1}{2}}$ $(H_{\frac{1}{2}}=1/\gamma(T_1T_2)^{\frac{1}{2}}$ where $H_{\frac{1}{2}}$ is the value of the microwave field H_1 which makes the ordinary saturation parameter $\frac{1}{2}$. V_R is plotted for various values of a. For the F center an estimate of a places it in the range 1.6×10^{-4} to 10^{-3}, indicating why the saturation curve of the F center is quite flat for $X\gg1$. Having an experimental saturation curve intermediate between the homogeneous and complete inhomogeneous case, it is now possible to relate the shape of the saturation curve to the individual spin-packet width ΔH_L.

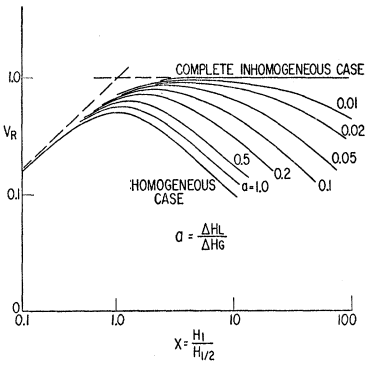

FIG. 1. Inhomogeneous saturation curves showing the spectrometer absorption signal V_R *versus* the reduced microwave field $H_1/H_{\frac{1}{2}}$, where $H_{\frac{1}{2}}=1/\gamma(T_1T_2)^{\frac{1}{2}}$ for various values of a. The quantity a is the ratio of the spin-packet width to inhomogeneous envelope width. These curves are a plot of (19).

Determination of T_2, $(T_1T_2)^{\frac{1}{2}}$, and T_1

Combining curve-fitting techniques with the results above, one can determine the spin-packet width and the spin-lattice relaxation time. Figure 2 shows a typical absorption signal saturation curve. We introduce now the quantities $V_{R\,\frac{1}{2}\,\text{lower}}$ and $V_{R\,\frac{1}{2}\,\text{upper}}$ where $V_{R\frac{1}{2}}$ is $\frac{1}{2}$ the maximum V_R for a given saturation curve. If we consider the separation between $V_{R\,\frac{1}{2}\,\text{upper}}$ and $V_{R\,\frac{1}{2}\,\text{lower}}$ as a measure of the width of the saturation curve it is evident from Fig. 1 that the width increases as the parameter a decreases. By taking the various

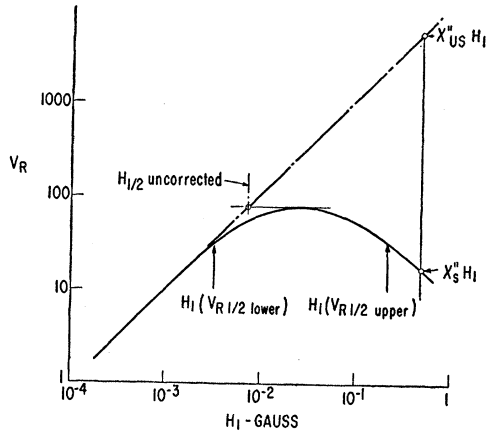

FIG. 2. Typical inhomogeneous saturation curve. The experimental ratio of $H_1(V_{R\,\frac{1}{2}\ \text{upper}})$ to $H_1(V_{R\,\frac{1}{2}\ \text{lower}})$ determines a or $\Delta H_L/\Delta H_G$ and hence T_2. $H_{\frac{1}{2}}$ is H_1 at the onset of saturation and determines $(T_1T_2)^{\frac{1}{2}}$. The ratio of $\chi_{us}''H_1$ to $\chi_s''H_1$ for $H_1 \gg H_{\frac{1}{2}}$ $(H_1 > H_{\frac{1}{2}}T_2/T_2^*)$ determines T_1 when T_2^* is known.

values of a in Fig. 1 and computing the ratio of H_1 $(V_{R\,\frac{1}{2}\ \text{upper}})$ to H_1 $(V_{R\,\frac{1}{2}\ \text{lower}})$, the curve shown in Fig. 3 is determined. From the value $H_1\,(V_{R\,\frac{1}{2}\ \text{upper}})/H_1\,(V_{R\,\frac{1}{2}\ \text{lower}})$ for a given experimental curve, it is possible with the help of Fig. 3 to obtain a and the individual spin-packet width. An appealing feature of this T_2 determination is that it does not require an absolute determination of H_1.

The evaluation of $H_{\frac{1}{2}}$ and consequently $(T_1T_2)^{\frac{1}{2}}$ can now be done once a has been found. The intersection of the linear signal below saturation with the horizontal line drawn tangent to the maximum of the saturation curve locates what we shall call $H_{\frac{1}{2}\ \text{uncorrected}}$. The multiplicative correction factor which relates it to the true $H_{\frac{1}{2}}$ is a known function of a (see Fig. 1) and ranges from 1 for a equal zero to 2 for the completely homogeneous case (for the homogeneous saturation case $H_{\frac{1}{2}}$ corresponds to $V_{R\ \max}$). We have now determined nearly independently T_2 and $(T_1T_2)^{\frac{1}{2}}$.

For $H_1 \gg H_{\frac{1}{2}}$ and $a \ll 1$ it is possible to determine T_1 independently by a method herewith called the T_2^* method. Here $T_2^*(\Delta\omega_G/\sqrt{2})=1$ if we note that $\Delta\omega_G/\sqrt{2}$ is just the rms static width of the inhomogeneous line. It can be shown (see Appendix B) that the ratio of the saturated absorption susceptibility to the unsaturated susceptibility is given by

$$\frac{\chi_s''(\omega_0)}{\chi_{us}''(\omega_0)}=\left(\frac{2}{\pi}\right)^{\frac{1}{2}}\frac{1}{\gamma^2H_1^2T_1T_2^*}$$
$$(1+\text{correction terms}), \quad (20)$$

where $1/\gamma^2H_1^2T_1T_2^*$ looks like an ordinary saturation parameter $(\gamma^2H_1^2T_1T_2^* \gg 1)$ in which T_2 has been replaced by T_2^* representing the static line width. We can say that Eq. (20) represents physically the saturation of the entire Gaussian distribution of spin packets, and the individual spin packet has lost its identity. However, for (20) to be valid it is necessary that $H_1 > H_{\frac{1}{2}}(T_2/T_2^*)$, which is a more restrictive condition than for a homogeneously broadened line of width T_2^* since we also require $a \ll 1$ for the correction terms to be small.

The picture of inhomogeneous saturation of χ'' is as follows. The onset of saturation of the individual spin packet occurs when H_1 approaches $H_{\frac{1}{2}}$. As H_1 increases above $H_{\frac{1}{2}}$, the absorption susceptibility of the spin packet falls off as $1/H_1^2$. However, as H_1 increases it is also covering more and more spin packets; in fact, the number of spin packets covered is closely proportional to H_1. Hence the susceptibility falls off as $1/H_1$ instead of as $1/H_1^2$. This $1/H_1$ falloff is not quite correct because, instead of having a constant distribution of spin packets, we have a Gaussian distribution of spin packets. The number of distinct spin packets is approximately $\Delta H_G/\Delta H_L$ or $1/a$. A word of caution should be injected about the spin-packet concept. If the spin-packet width arises from time-varying magnetic fields due to the reorientation of nuclear magnetic moments in the immediate vicinity of a center, two or more centers may belong to the same spin packet but still be essentially noninteracting. Finally, when H_1 approaches $(\Delta H_G/\Delta H_L)H_{\frac{1}{2}}$, enough power is available to saturate all the spin packets in the distribution, and the entire line then saturates homogeneously like a line of the static width.

Thus we can independently determine T_2, $(T_1T_2)^{\frac{1}{2}}$, and T_1 for an inhomogeneously broadened saturation curve, provided the saturation curve extends over a sufficiently large range of microwave power. The T_2 or spin-packet width is determined by the parameter a which is a function of the width of the absorption signal saturation curve. The value of $(T_1T_2)^{\frac{1}{2}}$ results from $H_{\frac{1}{2}}$ which measures the onset of saturation of the individual spin packet. It should be emphasized that each individual spin packet saturates homogeneously. Finally, by the "T_2^* method" where all the spin packets are saturated together much like a line of width $\Delta\omega_G=\sqrt{2}/T_2^*$, we can determine T_1. These three approaches will be applied to the saturation of V_K center ESR transitions. For the F-center case only the value

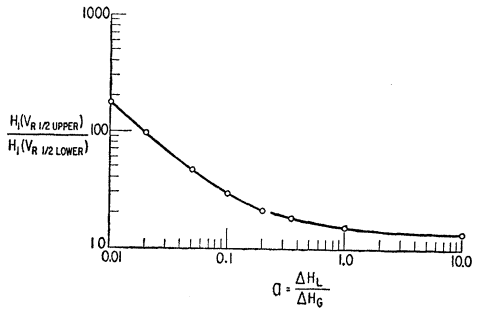

FIG. 3. The ratio of $H_1(V_{R\,\frac{1}{2}\ \text{upper}})$ to $H_1(V_{R\,\frac{1}{2}\ \text{lower}})$ *versus* a or $\Delta H_L/\Delta H_G$, based on curves shown in Fig. 1.

$(T_1T_2)^{\frac{1}{2}}$ or $H_{\frac{1}{2}}$ could be determined, because not enough of the saturation curve could be obtained.

The Experimental Apparatus and Techniques

The experiments reported here were done with an X-band spectrometer of the balanced-mixer type featuring a closed loop and separate sample cavity and detector magic-tee bridges. A block diagram of the spectrometer is shown in Fig. 4. An excellent analysis of various types of spectrometers is given by Feher.[12] This type of balanced-mixer closed-loop spectrometer has two significant advantages. First, klystron amplitude noise can be balanced out to first order by the use of matched detectors. Second, and of importance for saturation work, one can keep a constant microwave bias power on the detectors while the power incident on the sample cavity can be varied from maximum power to 100 db below maximum power. The conversion gain of the detectors remains constant while the power incident on the sample cavity is varied over many orders of magnitude. The klystron employed was a V58 with a maximum power output of 600–700 milliwatts for the high-power mode. The klystron was frequency-stabilized with a modified Pound I. F. Stabilizer.[13] For detectors selected Sperry 821 Bolometers were used. For independent microwave phase adjustment and microwave power attenuation a Hewlett Packard X885A Phase Shifter and a Hewlett Packard X382A Precision Variable attenuator were employed. The narrow-band amplifier was a Liston Becker 8-cycle breaker amplifier modified as follows. The input breaker was disconnected converting the amplifier into an 8-cycle ac amplifier. The input breaker served as the reference for the 8-cycle modulation of the magnetic field. The output breaker acted as a synchronous detector.

The sample cavity was operated as close to match as possible ($|\Gamma|<0.01$ was readily obtainable) meaning that the cavity bridge was nearly balanced. The bridge unbalance was monitored with a crystal connected to a sensitive galvanometer which could detect an unbalance of 0.01 microwatt. Because the power incident on the sample was varied over a 70-db range from 275 milliwatts down to 0.027 microwatt, it was necessary to have about 50 db isolation between the sample cavity and the microwave bias power (20 milliwatts) incident on the bolometers. The phase shifter was used to select χ'' or χ'. For strong saturation of χ'' the ratio of χ' to χ'' may be greater than 20 db, requiring accurate phase settings to better than 1°. This was achieved by modulating (temporarily) the klystron frequency at 8 cycles/sec after carefully tuning the klystron to the frequency of the sample cavity. Looking at the 8-cycle signal output of the Liston Becker Amplifier on a scope and tuning the phase shifter for a null of the 8-cycle signal, the phase can be accurately set for χ'', making use of the full sensitivity of the narrow-band detection scheme.

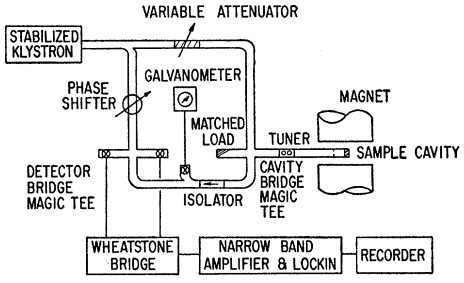

FIG. 4. The balanced-mixer spectrometer featuring a closed loop. Matched bolometers are used as detectors. Isolation between the detector bridge and the sample cavity bridge is important for low-power operation.

To determine the microwave field H_1 required the measurement of the microwave power and the Q of the cavity. The power incident on the sample cavity was measured with a hp 430C Power Meter. The Q of the matched cavity was measured by placing the cavity reflection curve on the scope and measuring the frequency difference of the half-power points ($Q_L=\nu_0/\Delta\nu$). For the matched cavity $2Q_L=Q_0$, where Q_0 is the unloaded Q. The experimental Q_0's varied from 4000 to 4500. The relationship yielding H_1 for the TE_{01} mode and a rectangular cavity of length C, height A, and volume V_c is

$$\frac{H_1^2V_c}{8\pi}\left[1+\left(\frac{C}{A}\right)^2\right]=\frac{Q_0P_c}{2\pi\nu_0}, \tag{21}$$

where P_c is the power incident on the matched cavity and ν_0 is the microwave frequency. The maximum error in the H_1 determination is about 15% coming primarily for the Q measurement. With the V 58 Klystron the maximum H_1 obtainable at full power was 0.7 gauss.

The samples were 0.060 in. thick and covered the end wall of the aluminum cavity. The samples were irradiated while at 78°K through the cavity end wall 0.020 in. thick with a 50-kv x-ray tube with tungsten target. The irradiation times varied from 8 to 20 hours producing 10^{16} to 2 or 3×10^{17} V_K centers. Preliminary experiments with crystals of various thicknesses showed that the filtering of the x-rays by the cavity end wall was sufficient to assure a homogeneous concentration of V_K centers.

Because of the field modulation combined with synchronous detection the spectrometer measured $d\chi''/dH$, i.e., the derivative of χ'' as the dc field was swept slowly. If transitions within the individual spin packet are adiabatic and if no fast passage effects occur, then the derivative at its maximum will be proportional to $\chi''(\omega_0)$. The condition most difficult to meet is the achievement of slow passage due to the modulation of the magnetic field. The slow-passage

[12] G. Feher, Bell System Tech. J. **32**, 449 (1957).
[13] R. H. Dicke and R. H. Romer, Rev. Sci. Instr. **26**, 915 (1955).

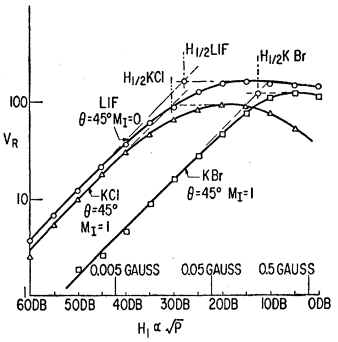

FIG. 5. Absorption saturation curves of the V_K center at 78°K in KCl, KBr, and LiF. ($V_R \propto \chi'' H_1$.) $H_{\frac{1}{2}}$ is give by $1/\gamma(T_1T_2)^{\frac{1}{2}}$ and measures the onset of saturation. θ is the angle between the external field and the V_K center axis, and M_I is the magnetic quantum number of the two nuclei making up the center.

condition is expressed by

$$\omega_m H_m < H_1/T_1, \tag{22}$$

where ω_m is the angular modulation frequency, and H_m is the modulation amplitude. However, fast-passage effects can only occur when the spin packet is saturated $[H_1 > 1/\gamma(T_1T_2)^{\frac{1}{2}}]$. Consequently, fast-passage effects will not occur if $\omega_m H_m < 1/\gamma T_1(T_1T_2)^{\frac{1}{2}}$. For the V_K center in KCl typical values of T_2 and T_1 at 78°K are 1 μsec and 7 μsec. With $\omega_m = 50$, slow passage requires $H_m < 50$ gauss, which is easily satisfied. It was possible in all the experiments at 78°K to avoid fast-passage conditions.

For a rectangular cavity and the TE_{01} mode, H_1 varies sinusoidally over the end wall. As a result, different centers "see" different H_1's and different parts of the crystal will begin to saturate at different powers. One should then integrate the signal V_R over the values of H_1 to which the V_K centers are exposed. Watkins[14] has shown that

$$\chi'' = \chi''(\omega_0, \langle H_1^2 \rangle_{Av}) \times \left[1 - \frac{X^2}{(1+X^2)^2} \frac{\langle [\Delta(H_1^2)]^2 \rangle_{Av}}{(\langle H_1^2 \rangle_{Av})^2} + \cdots\right], \tag{23}$$

where $X^2 = \langle H_1^2 \rangle_{Av}/H_{\frac{1}{2}}^2$ and $H_1^2 = \langle H_1^2 \rangle_{Av} + \Delta H_1^2$. The angular brackets indicate the average over the volume of the sample. Qualitatively one notices that the effect of a nonuniform H_1 is to flatten the saturation curve slightly at the peak. The effect then falls off for $X \ll 1$ and for $X \gg 1$. In these experiments a $\frac{5}{8}$-in. diameter shield was used during irradiation, restricting V_K center formation to the center two-thirds of the cavity. In this case the second term in the bracket for $X = 1$ is about 4%.

Experimental Results and Discussion

Steady-state ESR V_K center absorption saturation curves were obtained at 78°K in KCl, KBr, NaCl, and LiF with concentrations close to 10^{17} centers/cc. Because of the larger static line width and slower coloring rate not enough V_K centers could be obtained in NaCl to get a satisfactory signal-to-noise ratio over a large enough power range to obtain good saturation curves. The NaCl data will not be presented.

Figure 5 shows the absorption signal saturation curves for KCl, KBr, and LiF at 78°K. The ($\theta = 45°$, $M_I = 1$, LF) lines are shown for KCl and KBr while the ($\theta = 45°$, $M_I = 0$) line is shown for LiF. θ is the angle between the V_K center axis and the external magnetic field, M_I is the nuclear magnetic quantum number of the two nuclei making up the V_K center, and LF means lower external field than for the center ($M_I = 0$) line in contrast to HF for higher external fields than for the center line. The curves indicate that in KBr the absorption susceptibility starts to saturate with an H_1 an order of magnitude larger than required for saturation in KCl or LiF. The value of $H_{\frac{1}{2}}$ is slightly smaller for KCl than for LiF, indicating a slightly larger value of $(T_1T_2)^{\frac{1}{2}}$ for KCl than for LiF. However, the LiF absorption signal decreases only a small amount for $H_1 > H_{\frac{1}{2}}$ while for KCl the absorption signal bends down approaching a slope of -1 where $\chi'' \propto 1/H_1^2$ and $V_R \propto 1/H_1$. Qualitatively this implies that the V_K center in LiF has a smaller value of a or a smaller ratio of spin packet to static Gaussian width than in KCl. The LiF saturation curve does not remain as flat for $H_1 > H_{\frac{1}{2}}$ as it does for the F center because the V_K center resonance is less inhomogeneously broadened than the F-center resonance. Unfortunately, not enough microwave power was available to measure the saturation curve for KBr over a range that was sufficient to obtain T_2 and T_1 separately. Only the product T_1T_2 could be obtained for KBr.

Saturation curves were obtained for different hyperfine lines and for different values of θ. The detailed results will be presented first for KCl and KBr because of similar behavior and then for LiF because of its more complex behavior.

Figure 6 shows the absorption saturation curves of the V_K center in KCl in which both nuclei were Cl^{35} and a Cl^{35}-Cl^{37} center. In addition, the F-center absorption saturation curve is shown for comparison. The graph shows that the saturation curves for the 35-35 center and the 35-37 center are identical if we disregard the absolute intensity of the signal. In fact, data taken for all the lines in the hyperfine pattern for one θ have the same values of a and $H_{\frac{1}{2}}$ to within experimental errors (15%). Thus, within experimental error the

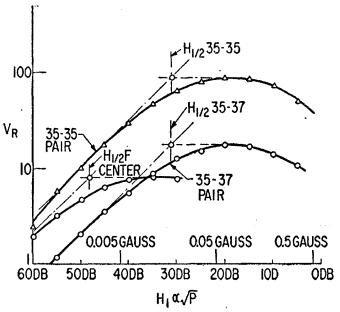

FIG. 6. V_K center absorption saturation curves for a Cl^{35}-Cl^{35} center and a Cl^{35}-Cl^{37} center at 78°K. An F-center absorption saturation curve at 78°K is also shown.

[14] G. Watkins, Ph.D. thesis, Harvard University (unpublished).

TABLE I. V_K center saturation parameters at 78°K.

	a	From a ΔH_L gauss	T_2 μsec	$H_{\frac{1}{2}}$ gauss	From $H_{\frac{1}{2}}$ $(T_1T_2)^{\frac{1}{2}}$ μsec	T_1 μsec	From T_2* T_1 μsec
KCl							
$\theta=45°$	0.052	0.049	1.0	0.019	2.6	6.8	6.2
$\theta=90°$	···	···	···	0.035	1.4	···	···
KBr							
$\theta=45°$	···	···	···	0.28	0.18	···	···
$\theta=90°$	···	···	···	>0.39	<0.14	···	···

lines, arising from different isotope combinations but corresponding to the same θ, have the same spin-packet width, and the same spin-lattice relaxation time. In KBr only $H_{\frac{1}{2}}$ could be determined from the saturation curves, but (as in KCl) it was the same to within the experimental error for all the hyperfine lines of a given θ for Br^{81}-Br^{81}, Br^{81}-Br^{79}, and Br^{79}-Br^{79} centers. Table I shows the results for KCl and KBr.

The Table indicates that T_1 is a factor of about six larger than T_2 for KCl at 78°K. The Table also indicates that the three determinations T_2, T_1, and $(T_1T_2)^{\frac{1}{2}}$ are consistent with one another to within the experimental error. It should be re-emphasized that the author was biased by previous work which suggested that the spin-packet width was T_1-limited. The data were first analyzed assuming $T_1=T_2$. This led to an inconsistency between the a method and $H_{\frac{1}{2}}$ method. It will be shown below that in LiF the inconsistency is an order of magnitude greater. In addition, when the data were first analyzed, the T_2* method for directly determining T_1 had not been considered. It was only after assuming $T_1\neq T_2$ that all the data could be satisfactorily explained. One also observes that the value $(T_1T_2)^{\frac{1}{2}}$ has a θ orientation dependence. For KCl at $\theta=90°$, $(T_1T_2)^{\frac{1}{2}}$ is about half the value measured at $\theta=45°$. Before attempting a complete understanding of the atomic processes contributing to T_1 and T_2, more data should be obtained for other values of θ and over a large temperature range. In LiF more extensive data were taken for different values of θ.

For the LiF V_K center, each different hyperfine line for a given θ behaves differently and we must explicitly specify the lines we are talking about. Figure 7 shows saturation curves for the $\theta=45°$, $M_I=1$ low-field (LF) line and the $\theta=45°$, $M_I=-1$ high-field (HF) line. The high-field line begins to saturate first; nevertheless, above saturation it does not bend down as quickly as the low-field line. Figure 7 also shows the saturation curve shapes, given $H_{\frac{1}{2}}$ and assuming $T_1=T_2$. The dashed extensions of the curves show what the assumption $T_1=T_2$ would do to the saturation curves. Here, even more dramatically than in KCl, the assumption $T_1=T_2$ is at variance with the experimental results.

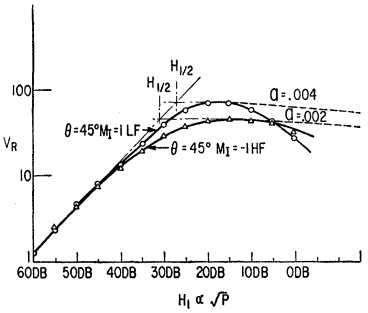

FIG. 7. V_K center absorption saturation curves in LiF at 78°K. Shown are high-field $M_I=-1$ and low-field $M_I=+1$ lines for $\theta=45°$.

Figure 8 shows more saturation curves for different θ and different hyperfine lines. The $\theta=90°$ doublet in LiF refers to the two small lines on the low-field side of the center line. There are two separate features of the saturation curves for LiF. First, for a given θ the LF lines always saturate less readily than the HF lines. In addition, the difference in saturation behavior of the LF and HF lines is large when these lines are far apart in field ($\theta=0°$) and small when these lines are close ($\theta=90°$ doublet). Secondly, there is also a complicated variation of the saturation behavior with θ. The onset of saturation occurs at lowest power for $\theta=0°$, and at highest power for $\theta=60°$. For $\theta=90°$ the saturation starts at a lower power than other angles except $\theta=0°$. Table II shows all the results and the saturation parameters.

Table II indicates spin-packet widths varying from 5 gauss down to $\frac{1}{4}$ of a gauss corresponding to T_2's varying from 0.01 μsec to 0.32 μsec, while the T_1's vary from about 15 to 45 μsec. For the LiF V_K center at 78°K the T_1's are much longer than the spin packet T_2's, the ratios varying from sixty to several thousand. The significant feature of the results is that T_2 depends in a complicated way on the dc magnetic field and on the angle θ between the field and the V_K center symmetry axis. T_2 values vary over a range of 30 while T_1 only varies over a factor of about 3. The difference in the magnitude of inhomogeneous broadening for the LF lines ($a>0.1$) and the HF lines ($a<0.1$) is apparent from the Table. The interpretation of these results for the individual spin-packet width ($1/\gamma T_2$) and for the spin-relaxation time T_1 using atomic processes will be undertaken in a future paper.

We can say the energy level pattern is different for high and low fields or for various θ. It is possible that nuclear spin mixing may be faster for one field or orientation than another. Abragam and Proctor have found that spin mixing depends on field.[15] The large

[15] A. Abragam and W. G. Proctor, Phys. Rev. **109**, 1441 (1958).

TABLE II. LiF V_K-center relaxation parameters at 78°K.

Run and line	a	Method a ΔH_L gauss	T_2 μsec	$H_{\frac{1}{2}}$ gauss	$H_{\frac{1}{2}}$ $(T_1T_2)^{\frac{1}{2}}$ μsec	T_1 μsec	T_2^* T_1 μsec	T_1/T_2
$\theta=0°$, $M_I=-1$ HF	0.021	0.18	0.28	0.014	3.6	48	···	170
$\theta=0°$, $M_I=1$ LF	0.16	1.4	0.036	0.048	1.0	30	41	830
$\theta=45°$, $M_I=-1$ HF	0.018	0.16	0.32	0.020	2.5	20		65
$\theta=45°$, $M_I=1$ LF	0.14	1.3	0.038	0.038	1.3	47	41	1200
$\theta=45°$, $M_I=0$	0.030	0.28	0.18	0.027	1.9	20	···	110
$\theta=60°$, $M_I=-1$ HF	0.085	0.74	0.068	0.048	1.0	16	···	240
$\theta=60°$, $M_I=1$ LF	0.56	4.9	0.010	0.076	.66	43	26	4200
$\theta=60°$, $M_I=0$	0.063	0.55	0.091	0.046	1.1	14	···	160
$\theta=90°$, $M_I=0$ HF	0.041	0.36	0.14	0.028	1.8	22	···	160
$\theta=90°$, $M_I=1$ LF	0.058	0.51	0.10	0.031	1.6	26	···	260
$\theta=90°$, $M_I=0$ HF	···	···	···	0.020	2.5	···	···	···

hyperfine interaction for the LiF V_K center and its large static-line width indicate that the nuclei neighboring the V_K center "see" quite different local fields, depending upon which hyperfine line, HF or LF, is being observed. It is further noted a spin-spin interaction between V_K centers cannot account for a T_2 which depends on field and angle θ.

Since completion of this paper, measurements have been made at the General Electric Research Laboratory with W. Känzig extending the data to 48°K, 20°K, and 11.5°K for KCl and LiF.[16] Experiments by pulse techniques have also been carried out in the liquid He range. In this forthcoming paper a development of the calculation of spin-lattice relaxation for the V_K center due to spin-orbit coupling, hyperfine coupling, etc., will be considered. Because the electronic structural properties and parameters of the center are well known (see C and K), it is felt that a reasonable comparison between the experimental relaxation times and calculated relaxation times can be attempted.

CONCLUSIONS

It is possible to treat the saturation of inhomogeneously broadened lines for the case in which the variation of the envelope distribution of spin packets over a single spin packet cannot be neglected. When the saturation curve can be measured over a sufficiently large power range, it is possible to determine separately the individual spin-packet width or T_2, $(T_1T_2)^{\frac{1}{2}}$, and the spin-lattice relaxation time, T_1. Saturation curves for the V_K center at 78°K indicate in KCl and LiF that the spin-packet width is not determined by T_1. T_1 may be much longer than T_2. For KCl all the hyperfine lines for a given θ have the same values of T_2 and T_1 to within experimental error. For KBr the product T_1T_2 is the same for all hyperfine lines of the same θ. In LiF T_2 is different for different hyperfine lines depending on both θ and H. In LiF T_1 depends on θ and may have a small H_0 dependence.

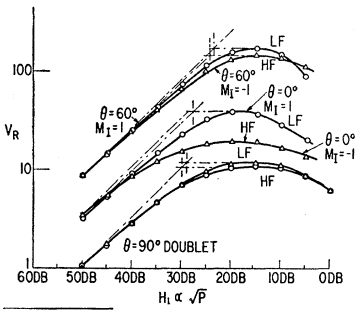

FIG. 8. V_K center absorption saturation curves in LiF at 78°K. The high-field and low-field lines for $\theta=60°$, $\theta=0°$, and $\theta=90°$ are shown.

[16] T. G. Castner, Bull. Am. Phys. Soc. 4, 21 (1959).

ACKNOWLEDGMENTS

Many stimulating discussions with Professor C. P. Slichter are gratefully acknowledged. Particular thanks are due to Dr. G. S. Newell for building the modified Pound I. F. Stabilizer and to Mr. W. C. Holton for aid in construction of components of the spectrometer. The author would like to thank Professor C. P. Slichter and Dr. W. Känzig for valuable suggestions concerning the manuscript.

APPENDIX A. EVALUATION OF THE INHOMOGENEOUS ABSORPTION SUSCEPTIBILITY INTEGRAL

The integral (17) is evaluated in the following way. One first introduces a set of reduced frequency variables $x_0=\omega_0/\Delta\omega_L$, and $x'=\omega'/\Delta\omega_L$ and, in addition, defines a saturation parameter s such that $s^2=\gamma^2H_1^2T_1T_2$. (17) becomes

$$\chi''(\omega_0)=\frac{\frac{1}{2}\chi_0 a}{\sqrt{\pi}}\int_0^\infty \frac{x'\exp[-a^2(x'-x_0)^2]dx'}{1+(x'-x_0)^2+s^2}. \quad (24)$$

Making the substitution $y=x'-x_0$ and (since $x_0>10^4$) replacing the lower limit $-x_0$ by $-\infty$, one obtains

$$\chi''(\omega_0)=\frac{\frac{1}{2}\chi_0 a}{\sqrt{\pi}}\int_{-\infty}^\infty \frac{(y+x_0)\exp(-a^2y^2)dy}{1+y^2+s^2}. \quad (25)$$

The first term in the integral vanishes because it is odd, leaving an integral, which will be designated $I(a,t)$, of the form

$$I(a,t)=2\int_0^\infty \frac{\exp(-a^2y^2)dy}{t^2+y^2}, \quad (26)$$

where $t^2=1+s^2$. This can now be written as

$$I(a,t)=2\exp(a^2t^2)\int_0^\infty \frac{\exp[-a^2(t^2+y^2)]dy}{t^2+y^2}. \quad (27)$$

Defining the integral in (27) as $J(a,t)$ and differentiating $J(a,t)$ with respect to a and evaluating the integral, one has

$$dJ(a,t)/da=-\pi^{\frac{1}{2}}\exp(-a^2t^2). \quad (28)$$

Next, integrating with respect to a, one obtains

$$J(a,t)=J(0,t)+\int_0^a [-\pi^{\frac{1}{2}}\exp(-a^2t^2)]da. \quad (29)$$

This integral has the form

$$J(a,t)=\frac{\pi}{2t}[1-\Phi(at)], \quad (30)$$

where $\Phi(at)=2/\pi^{\frac{1}{2}}\int_0^{at}\exp(-y^2)dy$, the usual error function. Combining (30) and (27) with (25), we obtain

$$\chi''(\omega_0)=\tfrac{1}{2}\chi_0\pi^{\frac{1}{2}}\left(\frac{\omega_0}{\Delta\omega_G}\right)\frac{\exp(a^2t^2)}{t}[1-\Phi(at)]. \quad (31)$$

APPENDIX B. SATURATION OF THE ENTIRE ENVELOPE OF SPIN PACKETS

The absorption susceptibility may be written in the form

$$\chi''(\omega_0)=\chi_0\left(\frac{\omega_0}{\Delta\omega_G}\right)\frac{\exp(a^2t^2)}{t}\int_{at}^\infty \exp(-x^2)dx. \quad (32)$$

If the substitution $y^2=x^2-a^2t^2$ is made, (32) will take the form

$$\chi''(\omega_0)=\chi_0\frac{\omega_0}{\Delta\omega_G}t\int_0^\infty \frac{y\exp(-y^2)dy}{[y^2+a^2t^2]^{\frac{1}{2}}}. \quad (33)$$

If $a^2t^2>1$ the denominator may be expanded in a Taylor's series, and the integral becomes

$$\frac{1}{at}\int_0^\infty y\exp(-y^2)\left[1-\frac{1}{2}\left(\frac{y}{at}\right)^2+\frac{3}{8}\left(\frac{y}{at}\right)^4-\frac{5}{16}\left(\frac{y}{at}\right)^6+\cdots\right]dy. \quad (34)$$

Integrating term by term, the saturated susceptibility becomes for $a^2t^2>1$

$$\chi_s''(\omega_0)=\tfrac{1}{2}\chi_0\frac{\omega_0}{\Delta\omega_G}\frac{1}{at^2}\left[1-\frac{1}{2a^2t^2}+\frac{3}{4a^4t^4}-\cdots\right]. \quad (35)$$

It is now convenient to evaluate $\chi''(\omega_0)$ when there is no saturation at all ($T_1=0$, yielding $t^2=1$). We start with

$$\chi_{us}''(\omega_0)=\chi_0\frac{\omega_0}{\Delta\omega_G}\exp(a^2)\int_a^\infty \exp(-x^2)dx. \quad (36)$$

This can be written as

$$\chi_{us}''(\omega_0)=\frac{\pi^{\frac{1}{2}}}{2}\chi_0\frac{\omega_0}{\Delta\omega_G}\exp(a^2)\left[1-\frac{2}{\pi^{\frac{1}{2}}}\int_0^a \exp(-x^2)dx\right]. \quad (37)$$

Expanding this for $a<1$ one obtains

$$\chi_{us}''(\omega_0)=\frac{\pi^{\frac{1}{2}}}{2}\chi_0\left(\frac{\omega_0}{\Delta\omega_G}\right)\left[1-\frac{2}{\pi^{\frac{1}{2}}}a+a^2-\frac{4a^3}{3\pi^{\frac{1}{2}}}+\cdots\right]. \quad (38)$$

One now takes the ratio of the unsaturated susceptibility $\chi_{us}''(\omega_0)$ found just above to the saturated susceptibility $\chi_s''(\omega_0)$, getting

$$\frac{\chi_{us}''(\omega_0)}{\chi_s''(\omega_0)}=\pi^{\frac{1}{2}}at^2\left[\frac{1-2a/\pi^{\frac{1}{2}}+\cdots}{1-\dfrac{1}{2a^2t^2}+\cdots}\right]. \quad (39)$$

But $t^2\gg1$ and hence $t^2\sim\gamma^2H_1^2T_1T_2$ and $a=\Delta\omega_L/\Delta\omega_G=T_{2*}/\sqrt{2}T_2$; consequently (39) becomes

$$\frac{\chi_{us}''(\omega_0)}{\chi_s''(\omega_0)}=\frac{\pi^{\frac{1}{2}}}{2}\gamma^2H_1^2T_1T_2^* \quad (1+\text{correction terms}). \quad (40)$$

If the correction terms are small, this expression is nearly independent of the spin-packet width $1/T_2$. Consequently, if the experimental conditions $a<1$ and $at>1$ can be satisfied, expression (40) may be used with an experimental saturation curve to determine T_1 directly. For KCl at 78°K the parameters for the V_K center of $a\sim0.05$ and $a^2t^2_{\max}\sim6$ correspond to $H_{1\max}\sim0.7$ gauss and the correction term will be about 3%.